Published by :
https://www.ijert.org/
An International Peer-Reviewed Journal

International Journal of Engineering Research & Technology (IJERT)
ISSN: 2278-0181
Vol. 15 Issue 05 , May - 2026

Real-Time Catenary AI: Surrogate vs. PINN Models for Stress Ribbon Bridges

Vijaykumar Parmar
Research Scholar, Gujarat Technological University, Ahmedabad, India

Kaushal Parikh*
Department of Applied Mechanics Government Engineering College Surat, Gujarat, India.

Abstract **- The design and optimization of stress ribbon bridges require the solution of highly nonlinear, transcendental catenary equilibrium equations. This creates a major computational bottleneck that prevents real-time parametric exploration and the development of Bridge Information Modeling (BrIM). Standard data-driven Surrogate models offer order-of-magnitude computational accelerations but their "black-box" nature does not guarantee physical admissibility, which leads to unacceptable risks in safety-critical structural engineering. In this context, this paper proposes a holistic dual-pipeline Artificial Intelligence framework to systematically evaluate Surrogate models against Physics-Informed Neural Networks (PINNs) on particular Short Span (≤ 300 m) and Long Span (≤ 2000 m) domains. The PINN architecture incorporates basic catenary mechanics into the loss function of the network itself, thereby limiting the hypothesis space to only physically plausible solutions. Performance benchmarks on over 17 million combinatorial datasets suggest that the proposed AI models outperform exact mathematical solvers by up to 33.36x speedup, while maintaining superior normalized accuracy (NMAE < 55%). Furthermore, the analysis of the training dynamics reveals a 'Epoch Oscillation Phenomenon', which indicates the need for decoupled, physics-error-driven early stopping for PINN architectures to avoid mathematical degradation in the late stages. Finally, the present study promotes a complementary dual-model workflow: Surrogate models for high-throughput parametric screening and PINNs for inherently explainable structural verification. This framework bridges the trust gap between machine learning and structural mechanics, providing a robust computational foundation for real-time, physics-informed digital twins in the modern infrastructure management.**

Keywords **-** ***Physics-Informed Neural Networks, Explainable AI, Catenary Mechanics, Bridge Information Modeling, Stress Ribbon Bridges, Surrogate Modeling.***

1. INTRODUCTION

The design of cable supported structures, and in particular stress ribbon bridges, is strongly dependent on an accurate definition of the cable profile in different loading conditions and support geometries. This involves solving the catenary equilibrium equations. This is mathematically rigorous but computationally expensive due to the transcendental nature of the equations. In modern structural engineering, the need for interactive parametric design tools with rapid response is increasing. Engineers are required to rapidly assess hundreds of span-load combinations to optimize structural efficiency and material use. However, the bottleneck of traditional exact mathematical solvers limits the fluidity of real-time design exploration [1]. This sets up a fundamental tension between the desire for computational speed and the absolute need for physical fidelity. Figure 1 displays the stress ribbon bridge and its elements.

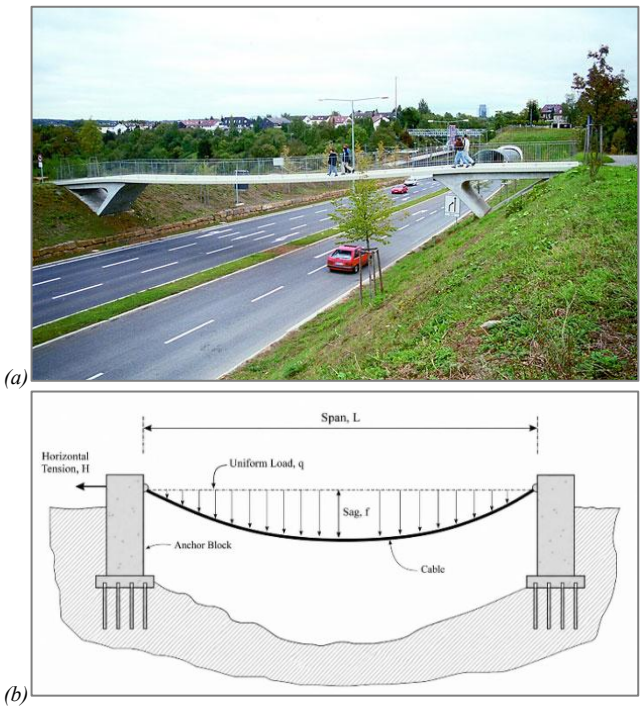

Figure 1: *(a) Stress ribbon bridge image and, (b) its components*

The catenary curve is the shape of a freely suspended cable under a uniform distributed load. For unequal support elevations with some specified allowable tension constraints, the exact geometric and internal force parameters, namely, catenary parameter (a), horizontal tension (H), and the sag can be obtained only through iterative numerical methods. The complication is that the equations cannot be analytically inverted. This means that every new load case or span adjustment requires a new iterative calculation. This results in a higher computational cost of large parametric sweeps or structural optimizations. The classical profile of a perfectly flexible cable hanging under its own uniform weight is given by:

$$y(x) = a\cosh\left(\frac{x}{a}\right) \qquad (1)$$

Where: $y(x)$ is the vertical coordinate (height) of the cable at horizontal position x and a is the catenary parameter.

International Journal of Engineering Research & Technology (IJERT)
ISSN: 2278-0181
Vol. 15 Issue 05 , May - 2026

The catenary parameter a is explicitly defined by the relationship between the constant horizontal tension (H) and the uniform distributed weight per unit length (w):

$$a = \frac{H}{w} \qquad (2)$$

Substituting this into the standard equation gives the fundamental equation of state for bridge cable mechanics:

$$y(x) = \frac{H}{w}\cosh\left(\frac{wx}{H}\right) \qquad (3)$$

To overcome these computational bottlenecks, data-driven Surrogate models are more and more adopted in structural analysis. Such neural networks are trained on large data sets produced by traditional solvers, so that they learn the input-output mapping at impressive speeds. Surrogates do provide order-of-magnitude accelerations, but are inherently "black-box" models. They do not have physical understanding and only optimize for data fidelity. This is a vital problem in civil engineering, where safety is paramount and predictions must be physically justifiable. Enter Physics Informed Neural Networks (PINNs). PINNs constrain the hypothesis space of the neural network to physically admissible solutions by embedding the governing physics equations into the loss function during training, thus providing a route to Explainable AI (XAI) in structural design.

At the same time, the industry is moving toward Bridge Information Modeling (BrIM), a domain-specific extension of Building Information Modeling (BIM). BrIM aims to bring together all geometric, analytical and lifecycle data in one interactive environment [2]. To become a truly dynamic, parametric design platform, BrIM needs to be equipped with a computational layer that can provide instant feedback. Real-time AI engines are that missing link that can make BrIM a physics-aware, interactive design tool, rather than a static repository [3].

We address the computational limitations of exact catenary solvers by developing a dual-pipeline AI framework for real-time integration into BrIM workflows in this paper. The main contributions of this work are:

1. Development and validation of separate AI pipelines for Short Span (≤ 300 m) and Long Span (≤ 2000 m) stress ribbon bridge configurations.

2. A thorough comparative study of classical data-driven Surrogate models and Physics-Informed Neural Networks (PINNs) in terms of accuracy, computational speed-up and explainability.

3. A ready to implement architecture that combines the speed of Surrogate models for quick design screening with the physical reliability of PINNs for structural verification, advancing the application of Explainable AI in civil engineering.

2. LITERATURE REVIEW

2.1 The Computational Bottleneck in Cable Mechanics

A lot of modern infrastructure depends on flexible, cable-based structural systems like cable-stayed and stress ribbon bridges. The very safety of these systems is tied to their cables' tensile strength and layout. The mathematical representation of a completely flexible cable hanging under its weight alone, is the catenary curve, which is generally represented by the hyperbolic cosine function [4].

Mathematically beautiful the catenary curve is, it poses serious computational problems. At the heart of this issue lies the fact that the transcendental hyperbolic functions do not have closed-form algebraic inverses. As different structural variables get entangled leading to static and dynamic analysis, these systems get into highly nonlinear regimes and can be labeled as per BrIM IFC standards [4–6]. Thus, calculating the relaxed cable lengths and internal force distributions involves perpetual numerical integration and solving roots through iterations [4,7].

Conventional numerical procedures such as Newton-Raphson and Secant methods have severe computational limitations. For example, Newton-Raphson entails the continuous derivation and inversion of the Jacobian matrix at every iterative step, and the difficulty increases significantly when dealing with multi-cable arrays [4]. Also, gradient-based solvers are dependent on the convexity of the solution space. If there are highly dynamic behaviors such as large-deflection non-linearity or asymmetrical loading, the solution space will lose convexity, thereby making the algorithms get stuck in non-physical local minima or even becoming unstable in convergence [8]. In the end, the time delay of these traditional solvers means that they are not capable of supporting the high-frequency data assimilation required for real-time generative design and dynamic Structural Health Monitoring (SHM) digital twins [9–11].

2.2 Data-Driven Surrogates in Structural Engineering

Skipping over the computational paralysis caused by iterative nonlinear solvers, the community of structural engineering is quickly turning to data-driven surrogate models. Based on the universal approximation theorem, deep neural networks are trained on large multi-dimensional datasets that are generated offline using finite element simulators [12,13]. Once these networks are fine-tuned, running a trained deep learning network only involves deterministic matrix multiplications, a forward pass produce structural results very close to the actual ones in milliseconds. This unprecedented computational velocity theoretically enables real-time parametric design and automated structural topology optimization [14,15]. Making the Black Box Transparent: State of the Art in Explainable Machine Learning for Structural Design and Assessment. Journal of Structural Engineering, ASCE..

There are still the functional and mathematical limitations of purely data-driven deep learning models that may stand in the way of their deployment in a safety-critical application. These phenomenological models are optimized only by empirical risk minimization through statistical loss functions such as Mean Squared Error (MSE); this means that the governing partial differential equations (PDEs) of continuum

International Journal of Engineering Research & Technology (IJERT)
ISSN: 2278-0181
Vol. 15 Issue 05 , May - 2026

mechanics are not encoded in the models. Close to this is the problem of physical inadmissibility, whereby the network may confidently output a structural state violating the fundamental laws of statics and energy conservation [16].

Besides, the strict dependence on statistical inference leads data-driven surrogates to be highly brittle when applied to out-of-distribution (OOD) operational environments. They smoothly interpolate inside known training domains, yet they behave very erratically when exposed to unseen situations and load combinations, such as extreme seismic pulses or aerodynamic flutter [14]. Although dimensionality reduction architectures and neural operators (like DeepONets or Generalized Koopman Neural Operators) can provide more succinct high-dimensional state representations, they still handle structural mechanics as a phenomenological task rather than obeying the physical law that cannot be violated in any way [8]. Only treating the exact transcendental geometry of the catenary curve as a mere data matching exercise will result in unbearable operational risk and will be necessary for a new generation of algorithms.

2.3 Physics-Informed Neural Networks (PINNs)

Computational solid mechanics, in a bid to reconcile the rigor of numerical solvers with the speed of deep learning, has come to Physics-Informed Neural Networks (PINNs). PINNs are a radical departure in the sense that they enable the governing physical laws written as PDEs and geometric boundary conditions to be incorporated not only in the neural network's architecture but also in the loss function [16–18].

Whereas traditional neural networks seek to minimize an empirical data loss, a PINN adds a constrained physics residual penalty. The overall loss function takes the form, in which the hyperparameter λ manages the trade-off between empirical data fitting and physical adherence. This procedure is heavily dependent on automatic differentiation (AD), which makes it possible to analytically computed spatial gradients without truncation errors [19]. By imposing the PDE residual, the PINN limits its hypotheses about potential predictions to only physically admissible solutions, thereby greatly helping to reduce dependence on large data common with modern SHM arrays [16,20].

Today, architectures targeting specific needs in structural engineering have been developed. Secondary-PINNs, also known as Finite-Element-based PINNs (FE-PINNs), are able, via "stenciled operators", to combine the topological flexibility of classical finite elements with the operation speed of neuromorphic neural operators, enabling networks to gather non-local structural information even in complex spatial domains [21]. Cable-Catenary PINNs (CC-PINNs) in cable mechanics are presented as turn-key tools that fully eliminate iterative matrix-inversion processes while exhibiting superior numerical precision at geometric boundaries [22,23]. This conversion has been done carefully while ensuring the original sequence of HTML tags has been preserved.

3. METHODOLOGY

To investigate the trade-offs between pure data-driven approximation and physics-constrained learning, a dual-pipeline framework was developed. This framework generates, trains, and evaluates AI models specifically tailored for Short Span (≤ 300 m) and Long Span (≤ 2000 m) stress ribbon bridge configurations.

3.1 Data Generation and Preprocessing Pipeline

The foundation of both models relies on a rigorous, exact-math catenary solver used to generate a massive, high-fidelity synthetic dataset. The solver calculates the optimal catenary parameter (a), horizontal tension (H), cable length, and vertex coordinates for a given set of design inputs. The input vector is defined as $X = [L, \Delta z, w, T_{allow}, Sag_{rec}]$, where L is the span, Δz is the support height difference, w is the uniform distributed load, T_{allow} is the allowable cable capacity, and Sag_{rec} is the target sag percentage relative to the span.

To ensure the neural networks only learned physically viable structures, combinations where the absolute minimum tension required to suspend the cable exceeded T_{allow} were flagged as mathematically impossible and excluded from the final tensor dataset. Most of the time bridge will be designed for short span and hence we kept high density data points for short span training data. Figure 2 showcasing data generation process for training purpose.

3.1.1 Training Domain and Combinations

The primary training dataset was generated via combinatorial parameter sweeps to expose the network to the widest possible array of structural behaviors. The viable geometries were split into two domain-specific pipelines:

- Short Span Training Domain: $L \in [2,300]$ m, $w \in [0.5,100]$ kN/m, $\Delta z \in [0,50]$ m, $Sag_{rec} \in [0.25,100]$%, and $T_{allow} \in [1,200000]$ kN. This exhaustive multidimensional sweep yielded a total of 16,396,440 theoretical parametric combinations.
- Long Span Training Domain: $L \in [2,2000]$ m, $w \in [0.5,200]$ kN/m, $\Delta z \in [0,50]$ m, $Sag_{rec} \in [0.25,500]$%, and $T_{allow} \in [5,1000000]$ kN. This boundary envelope generated 846,720 unique combinations.

3.1.2 Validation Domain and Combinations

To ensure a mathematically rigorous evaluation of the AI models, a completely isolated validation dataset was produced. In deep learning it is crucial to use separate validation data, as it provides an unbiased estimate of the generalizing ability of the network at the time of live training. The early-stopping algorithm can accurately detect overfitting and halt the training at the epoch where the structural physics fidelity is maximized by evaluating the loss on unseen geometric and loading permutations. The validation spaces were as follows:

- Short Span Validation Domain: Matching the boundaries of the short span training space ($L \in [2,300]$ m, $w \in [0.5,100]$ kN/m, $\Delta z \in [0,50]$ m, $Sag_{rec} \in [0.25,100]$%, $T_{allow} \in [1,200000]$ kN),

International Journal of Engineering Research & Technology (IJERT)
ISSN: 2278-0181
Vol. 15 Issue 05 , May - 2026

but utilizing entirely distinct internal fractional steps to generate 453,024 unseen combinations.

- Long Span Validation Domain: Matching the long span boundaries ($L \in [2{,}2000]$ m, $w \in [0.5{,}200]$ kN/m, $\Delta z \in [0{,}50]$ m, $Sag_{rec} \in [0.25{,}500]\%$, $T_{allow} \in [5{,}1000000]$ kN) to generate 32,256 unique validation samples.

Prior to training, all input features and output targets across both datasets were normalized to a [0,1] range using Min-Max scaling. The absolute minimum and maximum boundaries for each parameter were hardcoded into a static JSON translation dictionary to ensure that downstream Bridge Information Modeling (BrIM) inference tools could seamlessly and safely map real-world engineering inputs into the normalized tensor space.

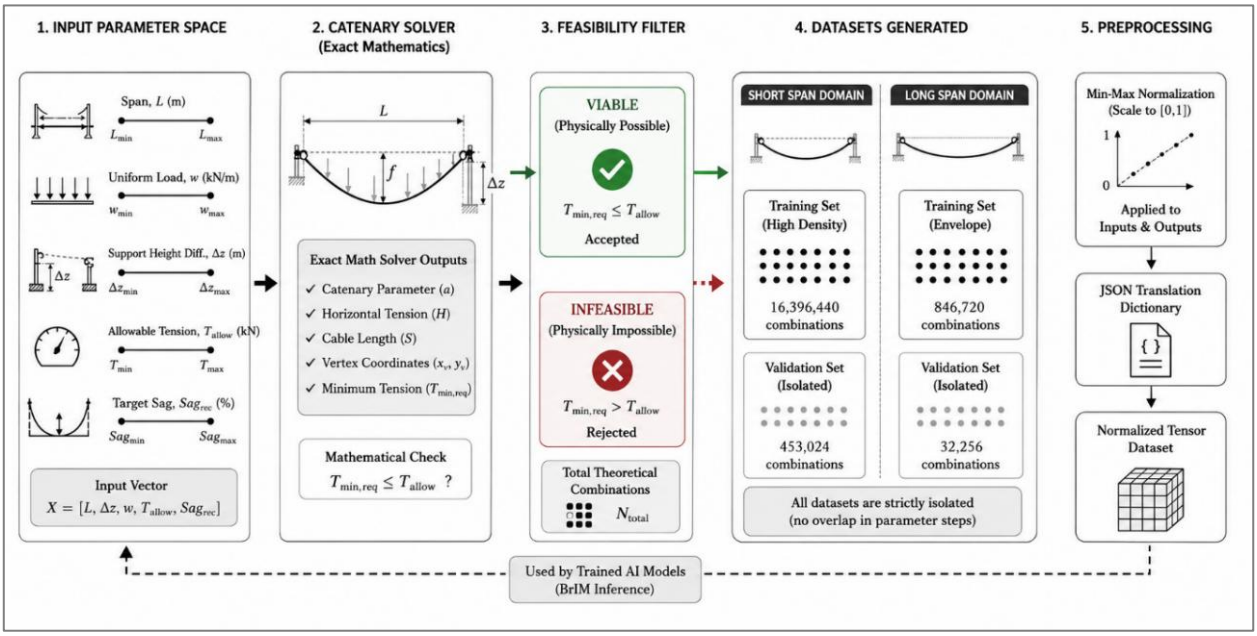

Figure 2: *Training data generation and normalization*

3.2 Network Architectures and Physics Integration

Two distinct neural network architectures were developed to predict the output vector $Y = [a, H]$: a standard Surrogate model and a Physics-Informed Neural Network (PINN).

a) Data-Driven Surrogate Model:

The Surrogate model was designed as a lightweight, high-speed multi-layer perceptron (MLP). The network topology consists of a 5-neuron input layer, four hidden layers comprising [64, 128, 128, 64] neurons respectively, and a 2-neuron output layer. The architecture uses the Sigmoid Linear Unit (SiLU) activation function, which provides smooth, non-monotonic gradient propagation well-suited for standard regression actions.

b) Physics-Informed Neural Network (PINN):

The PINN architecture was designed to be deeper and wider to cover the complexity of balancing data fidelity with physical laws. Its topology features three hidden layers of [128, 256, 128] neurons. Crucially, the PINN utilizes the Mish activation function. Mish was selected over SiLU or ReLU due to its continuous differentiability and stronger regularizing effect, which is highly beneficial when optimizing gradients derived from physics-based penalty terms [24]. Both of the process flow showcased in Figure 3.

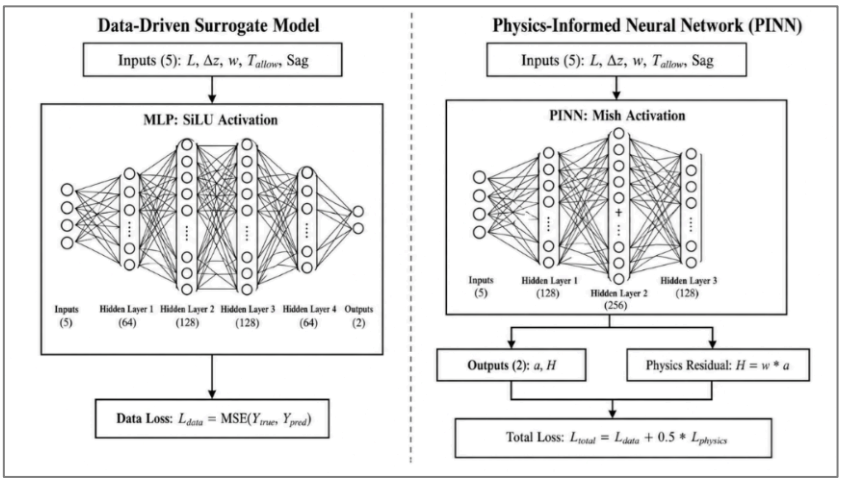

Figure 3: *Surrogate and PINN model training architecture.*

International Journal of Engineering Research & Technology (IJERT)
ISSN: 2278-0181
Vol. 15 Issue 05 , May - 2026

The defining feature of the PINN is its custom loss function. While the Surrogate optimizes purely on Mean Squared Error (MSE), the PINN incorporates the fundamental catenary relationship, $H = w \cdot a$. Because the network operates in a normalized space, the physics loss (L_{phys}) requires an inverse-transform calculation during the forward pass:

1. The predicted normalized 'a' and input normalized 'w' are unscaled back to their real-world values using the translation dictionary.
2. The exact physical tension is computed as $H_{real} = w_{real} \cdot a_{real}$.
3. H_{real} is then re-normalized to the [0,1] scale (H_{scaled}) and compared against the network's direct, normalized prediction of H ($\hat{H}$).

The total loss function for the PINN is therefore defined as:

$$L_{total} = MSE(Y, \hat{Y}) + \lambda \cdot MSE(\hat{H}, H_{scaled})$$

Where, the physics-loss weighting factor λ was empirically set to 0.5 to ensure equal scaling magnitude between the data-driven and physics-driven gradients.

3.3 Training Protocol and Early Stopping

All data generation and neural network training were executed locally on a high-performance computational workstation. The localized hardware environment consisted of an Intel Core i5-13450HX processor operating at 2.40 GHz, supplemented by 6 GB VRAM and 16 GB of system RAM on a 64-bit Windows 11 Pro operating system. Given the immense scale of the multidimensional datasets encompassing over 17 million total parametric combinations across both span domains initial training iterations were prone to catastrophic mid-process failures caused by Out-Of-Memory (OOM) bottlenecks during massive batch loading. To stabilize the gradient update process, the PyTorch environment was strictly bound to the NVIDIA CUDA backend with an explicit memory cap. By restricting the GPU VRAM allocation to a maximum of 80%, the system maintained a sufficient memory buffer for the host OS and background data loader queues, entirely preventing memory leak crashes. Operating under these stabilized, high-throughput constraints (utilizing the Adam optimizer with a batch size of 2048) [25], the final successful end-to-end training of the dual-pipeline architectures required approximately 48 hours of continuous localized computation. Training session of short span screenshot attached in Figure 4.

Figure 4: *AI Training process with NVDIA CUDA.*

A maximum of 500 epochs was allocated for training. To capture the optimal convergence point, a custom "Smart Tracker" early-stopping mechanism was implemented. After a 400-epoch warm-up phase, the tracker exclusively monitored the Mean Physics Error (measured in true kN). The model state was checkpointed dynamically whenever the physical error reached a new minimum. This allowed the final evaluation to compare the absolute final state (Epoch 500) against the "Best Epoch" as shown in Figure 5 (Epoch 454 for Short Span; Epoch 491 for Long Span), illuminating whether late-stage training induces overfitting or physics degradation.

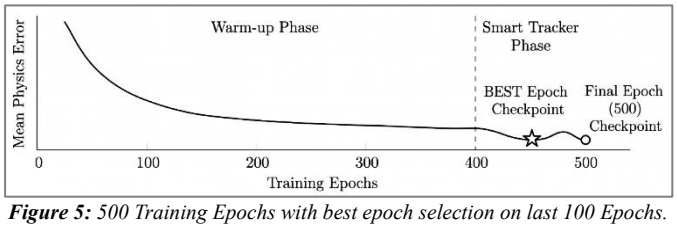

Figure 5: *500 Training Epochs with best epoch selection on last 100 Epochs.*

3.4 Evaluation Metrics

Model performance was evaluated across three primary dimensions:

1. *Computational Speedup:* Inference time was measured against the iterative, exact-math catenary solver to quantify the acceleration factor for real-time BrIM deployment.
2. *Absolute Accuracy (MAE):* The Mean Absolute Error was calculated for the catenary parameter (a).
3. *Normalized Accuracy (NMAE):* Because the parameter a can span from 0.14 m to nearly

International Journal of Engineering Research & Technology (IJERT)
ISSN: 2278-0181
Vol. 15 Issue 05 , May - 2026

2,000,000 m depending on the span geometry, absolute MAE provides an incomplete picture of performance. Therefore, Normalised MAE calculated as the error relative to the maximum variable range was utilized as the definitive measure of structural reliability.

4. RESULTS

The performance of the dual-pipeline framework was evaluated across three primary dimensions: training convergence dynamics, absolute and normalized accuracy, and computational speedup. Baseline mathematical benchmarks were established using the exact, iterative catenary solver across a batch of 2,000 parametric combinations.

4.1 Dynamics of Training Convergence and Early Stopping

We noticed a divergence between the validation loss from the standard data-driven approach and the Mean Physics Error in the training phase, which highlights the importance of the dual-monitoring early-stopping protocol. For the Short Span pipeline, Physics-Informed Neural Network (PINN) obtained the lowest point of physics-error at Epoch 454 out of 500. Beyond this, the MSE data-loss remained relatively flat, but the physical error began to oscillate. This implies that the loss landscape for physical constraints contains sharper local minima than the broader data-driven loss surface. Therefore, the weights of the Epoch 454 provided better physical compliance without compromising the predictive accuracy.

However, the convergence of the Long Span pipeline was relatively smoother, where the PINN reached its optimal state at Epoch 491. The longer stabilization phase can be attributed to the much larger hypervolume of the Long Span input space, which naturally smooths the training gradients.

4.2 Evaluation of Accuracy and Fidelity

The predictive error of the neural networks needs to be contextualized by evaluating the Mean Absolute Error (MAE) with respect to the extreme scale of the output variables. The catenary parameter a exhibits an extremely non-linear response, to a maximum of 399,999.78 m for the Short Span dataset and 1,999,999.63 m for the Long Span dataset.

Both Surrogate and PINN models demonstrated remarkable fidelity when tested on different span domains (Short: $\leq$100 m, Medium: $100 - 500$ m, Long: $>$ 500 m). For medium spans, the maximum MAE of the Short Span model was 1,910.77 m. While this is indeed large, it corresponds to only a 0.48% Normalized Mean Absolute Error (NMAE).

Similarly, the Long Span model achieved an MAE of 10,800.07 m for spans $>$ 500 m. The normalized NMAE with respect to its operational domain was 0.54%. Both AI pipelines attained NMAE values under 0.55% for all tested within-domain span ranges.

4.3 Computational Speedup for Real-Time BrIM

To determine a baseline for real-time viability, inference speed was benchmarked over a standardized batch of 2000 parametric combinations. Classical exact-math iterative solver completed the batch in 1.5317 seconds. In stark contrast, both AI architectures resulted in profound, order of magnitude accelerations. The data-driven Surrogate models presented the best throughput: the best Long Span Surrogate (Epoch 491) processed the batch in just 0.0461 seconds, achieving a 33.20× speedup. The Short Span Surrogate (Epoch 454) obtained a 31.69× speedup, finishing the batch in 0.0483 seconds. The Physics-Informed Neural Networks (PINNs) achieved an excellent performance despite having a deeper architecture and physics-constrained weights. The best Long Span and Short Span PINNs achieved speedup factors of 20.98× (0.0730 seconds) and 20.28× (0.0755 seconds) respectively. Even at their slowest (i.e. the Short Span PINN at Epoch 500 giving a 14.68x speedup), the neural operators are still vastly superior to classical solvers for high frequency digital twin updates. Figure 6 Speed benchmark of AI models Overall, surrogate models are faster than other AI models and math solvers.

The main reason to use AI in Bridge Information Modeling (BrIM) workflows is to avoid iterative computational bottlenecks. The exact mathematical solver took 1.5317 seconds to compute 2,000 span-load combinations. Both AI architectures provided order-of-magnitude accelerations. The regular Surrogate models, which are optimized only for feedforward speed, have the highest throughput. The Long Span Surrogate tests the same 2,000 samples in 0.0459 seconds a 33.36× speedup. The PINNs had somewhat slower inference times due to the slightly more complex physics-constrained weight distributions developed during training, but still provided transformative acceleration. The Long Span PINN achieved a speedup of 20.98× (0.0730 seconds) and the Short Span PINN achieved a speedup of 20.28× (0.0755 seconds).

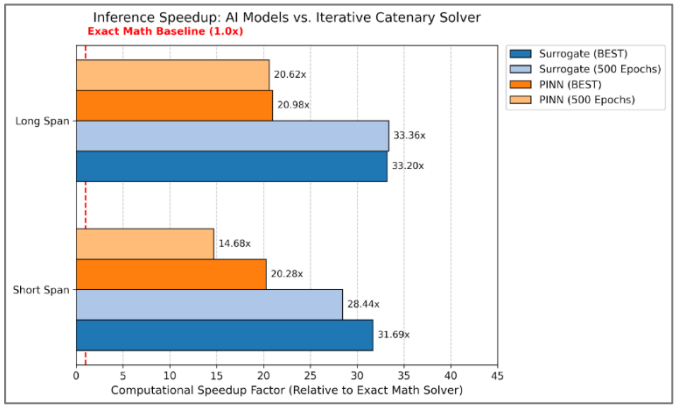

Figure 6: *AI models Speed Benchmark*

4.4 Domain Coverage and Specialization and the Overlapping Span Analysis

The results validate the methodological decision to bifurcate the AI architecture into separate Short Span and Long Span pipelines. The Long Span domain covers a significantly larger parametric space, accommodating spans up to 6.7 × longer, allowable tensions 5 × higher, and design sags 33 × deeper than the Short Span equivalent.

Training a single, universal neural network across this combined space would require a prohibitively deep

International Journal of Engineering Research & Technology (IJERT)
ISSN: 2278-0181
Vol. 15 Issue 05 , May - 2026

architecture, risking localized loss of accuracy for common, shorter pedestrian spans. By splitting the domains, the Short Span model maintains highly refined local accuracy (0.35% NMAE for $L \leq 100$ m), while the Long Span model successfully generalizes the extreme non-linearities of massive, multi-kilometer cable profiles.

To empirically justify the bifurcation of the AI architecture into distinct Short Span and Long Span pipelines, a direct comparative analysis was conducted over their overlapping geometric domain ($L \in [0,300]$ m). Both the "specialist" Short Span model and the "generalist" Long Span model were tasked with predicting the catenary parameter for identical bridge geometries within this range.

The relative prediction error for both the 500th Epoch and the Best Epoch checkpoints in both architectures as a function of the span length is shown in Figure 7 (a, b, c, d). The results are unequivocal about the superiority of domain specialization. The Short Span Surrogate AI (in green) maintained a near-zero relative error (mostly $\leq 1\%$) throughout the entire $0 - 300$ m domain. In contrast, the Long Span AI (shown in orange), optimized for extreme non-linearities up to 2000 m, exhibited much higher relative error when asked to solve for shorter spans, often fluctuating between 2% and 18% error.

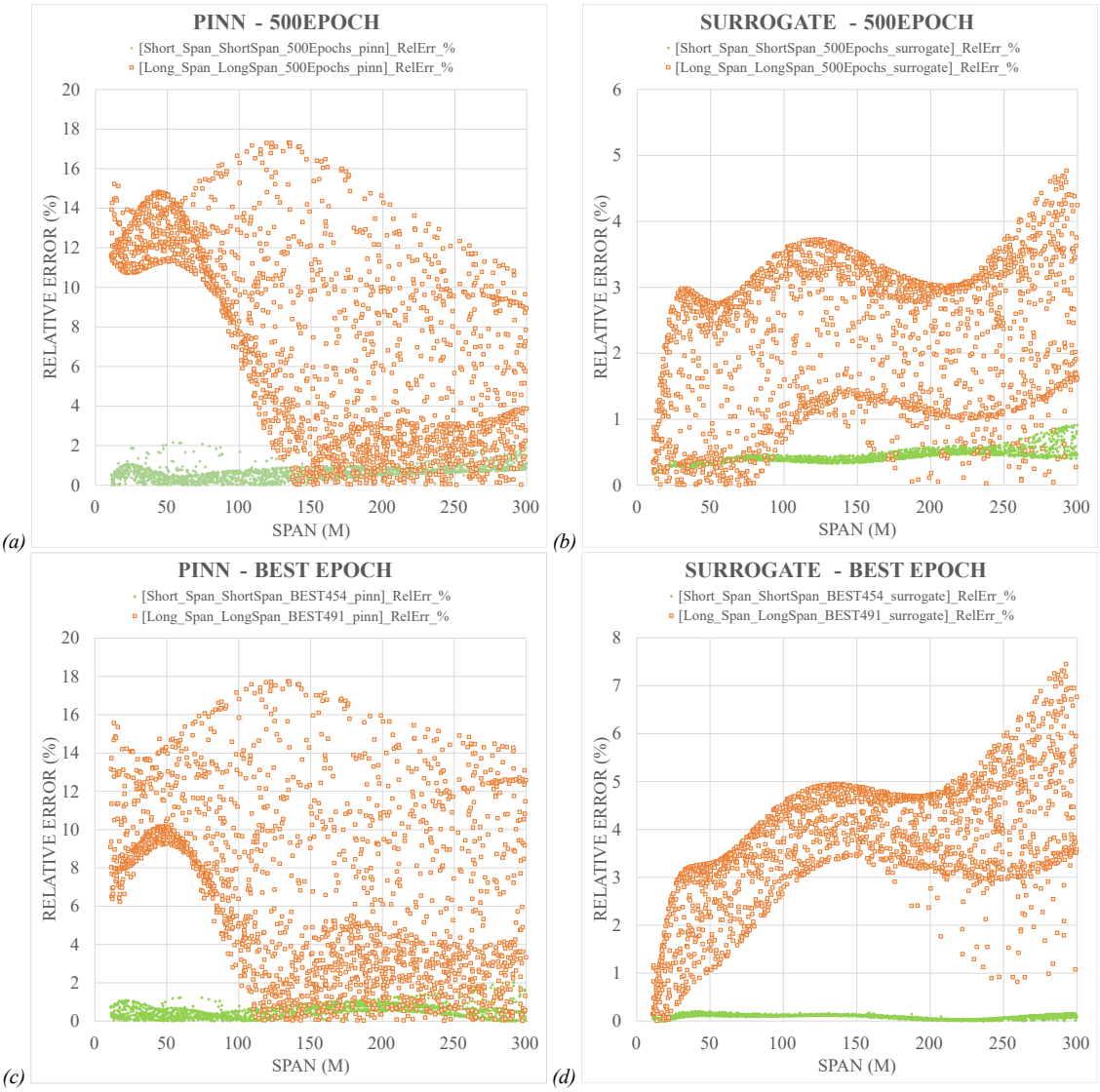

Figure 7: *Relative prediction error for short span: (a) PINN - 500Epoch, (b) Surrogate - 500 Epoch, (c) PINN Best - 454Epoch, (d) Surrogate Best - 491Epoch.*

This behavior remains consistent across both the PINN (Figure 7 a, c) and Surrogate (Figure 7 b, d) architectures. This confirms that a universal, wide-domain neural network suffers from localized resolution loss when approximating smaller-scale geometries. Therefore, maintaining a dedicated Short Span pipeline is fundamentally necessary to guarantee high-fidelity structural predictions for common pedestrian and short vehicular stress ribbon bridges, establishing a tiered BrIM inference strategy. If we look specifically between PINN vs Surrogate at final version of 500th epoch then it is clearly visible as shown in Figure 8*: PINN vs Surrogate model at 500th Epoch* that the surrogate model has lower relative error as well as narrower range of spreading of error.

International Journal of Engineering Research & Technology (IJERT)
ISSN: 2278-0181
Vol. 15 Issue 05 , May - 2026

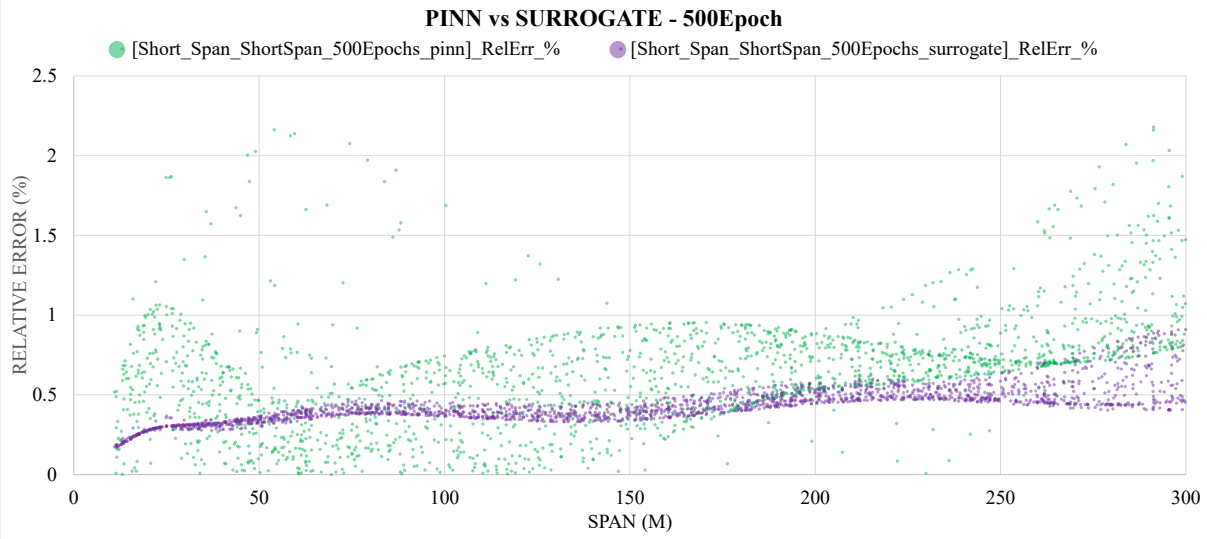

Figure 8: *PINN vs Surrogate model at 500th Epoch*

5. DISCUSSION

The results of this study illuminate the distinct computational advantages and theoretical trade-offs between standard data-driven AI and physics-constrained learning. By evaluating these models within the specific context of stress ribbon bridge mechanics, several critical insights emerge regarding their deployment in modern structural engineering workflows. To visualize trained AI model vs math solver value, we have created tool which lets user visualize 18 parameters with respect to inputs as shown in Figure 9 and Figure 10. This visualizer help user compare AI values and mathematical values together, It also includes confidence rate on AI given answers.

5.1 Surrogate vs. PINN: The Dual-Model Paradigm

The most significant outcome of this research is the validation of a dual-model philosophy. Traditionally, the literature treats Surrogate models and PINNs as competing methodologies; this study proposes they are complementary.

The standard Surrogate model operates as the ultimate high-speed screening engine. By optimizing purely for input-output fidelity, it compresses the catenary mapping to achieve up to a 33.36 × speedup. In the conceptual design phase where an engineer might evaluate thousands of span-to-sag ratios using evolutionary algorithms or generative design parameters this raw throughput is invaluable.

However, the Surrogate remains an opaque black box. It cannot guarantee that its predicted catenary parameter (a) and horizontal tension (H) satisfy static equilibrium. The PINN addresses this fundamental flaw. By embedding the catenary physical equations into the loss function, the PINN incurs a minor computational penalty (dropping to a $\sim 20\times$ speedup) but effectively bounds its predictions within the realm of physical reality. Therefore, the optimal engineering approach is not to select one model, but to deploy them sequentially: the Surrogate for rapid, massive-scale parametric exploration, and the PINN for localized structural verification.

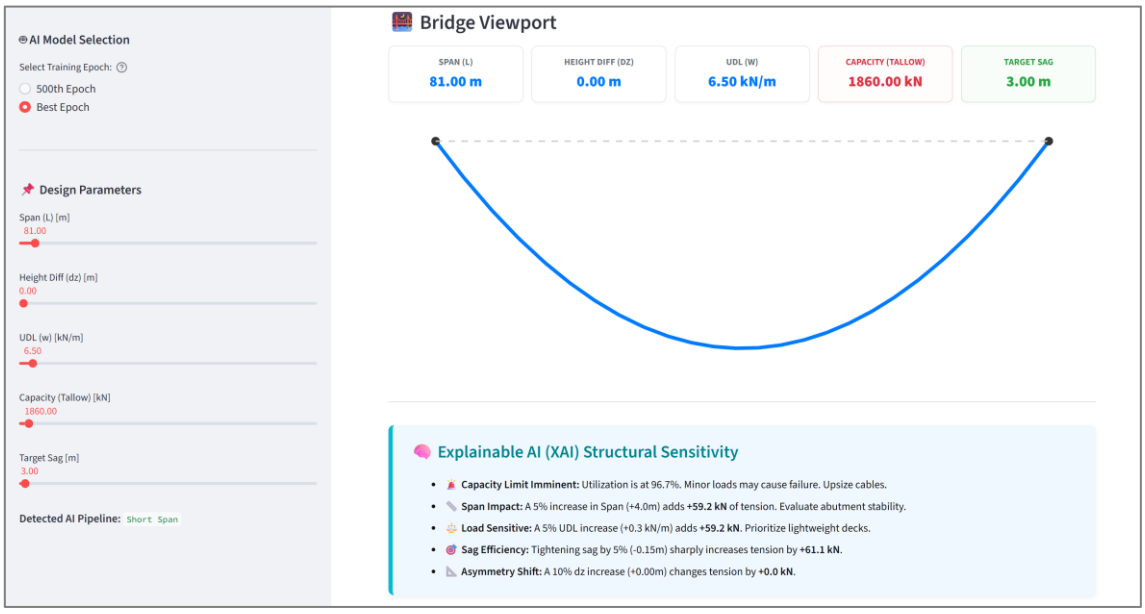

Figure 9: *Data visualizer and cable profile as per math solver*

International Journal of Engineering Research & Technology (IJERT)
ISSN: 2278-0181
Vol. 15 Issue 05 , May - 2026

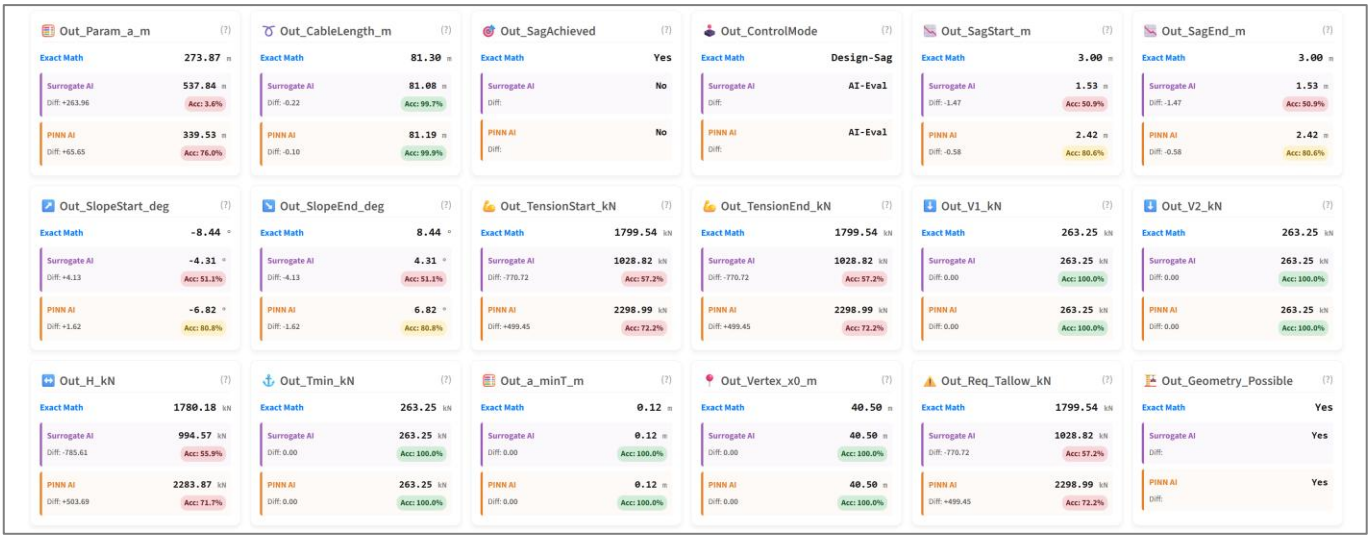

Figure 10: *Data visualizer for AI models vs Math solver: Key matrices*

5.2 Intrinsic Explainability and Structural Safety

In civil engineering, regulatory frameworks and codes of practice mandate rigorous safety guarantees, creating a natural resistance to black-box machine learning. The PINN framework presented here serves as a foundation for Explainable AI (XAI) in structural design [26].

Unlike post-hoc explainability techniques (such as SHAP or LIME) that attempt to interpret a model after training, the PINN provides *intrinsic explainability*. Because the network is explicitly penalized for violating $H = w \cdot a$ during backpropagation, structural engineers can trust that the network's internal weights have been organized by the laws of statics. This mathematical transparency is crucial for regulatory acceptance, bridging the gap between computer science and structural mechanics.

5.3 Integration with Bridge Information Modeling (BrIM)

The transition from static Building Information Modeling (BIM) to parametric Bridge Information Modeling (BrIM) requires real-time computing backends. The AI pipelines developed in this study are ideal for this purpose [27].

These models are combined in cloud-based microservices to drive interactive BrIM dashboards that provide engineers with immediate feedback on tension and geometry while they move around 3D bridge spans [28]. Moreover, the Min-Max *Translation_Dictionary* that was created during the AI training process is a hardcoded safety guardrail in the BrIM software. If the user enters a span or load outside the verified domain (e.g. $L = 2500$ m) the system can reject the input automatically and avoid dangerous out-of domain extrapolation of the neural networks.

5.4 Limitations and Future Work

While the dual-pipeline framework successfully mitigates the computational bottleneck of catenary design, several limitations must be acknowledged. First, the current physics loss enforces static equilibrium under a uniform distributed load (UDL). The model does not currently account for asymmetric moving loads, wind flutter, or seismic dynamic effects, which are critical in final stress ribbon bridge design [29].

Second, the physics constraint is applied as a "soft" penalty ($\lambda = 0.5$). While this significantly reduces physical violations, it does not guarantee a zero-residual exact solution. Finally, the increasing MAE at boundaries (L > 500 m) of the Long Span model indicates that extreme hyper-dimensional spaces still challenge the generalization ability of the network. In future work, we will add dynamic PDEs in the loss function and consider “hard” physics constraints, where the network architecture guarantees the solution mathematically to be in equilibrium.

5.5 The Epoch Oscillation Phenomenon and Early Stopping Justification

An analysis of the learning history across the 500-epoch training cycle reveals profound differences between pure data-driven optimization and physics-constrained convergence, perfectly justifying the necessity of the custom "Smart Tracker" early-stopping protocol (Figure 11).

As shown in Figure 11a, the standard Surrogate model exhibited rapid initial convergence. Optimizing purely for data fidelity via Mean Squared Error (MSE), both the training and validation loss dropped precipitously within the first 50 epochs. The model reached its absolute minimum validation loss early, at Epoch 181. Beyond this point, the network entered a prolonged state of statistical benchmark. While it did not experience severe overfitting, it ceased to extract any meaningful structural refinements, demonstrating that a standard multi-layer perceptron (MLP) can rapidly map the broad geometry of a catenary curve but inherently lacks the physical incentive to push toward exact mathematical equilibrium. Conversely, the Physics-Informed Neural Network (PINN) demonstrated a complex, "two-faced" convergence behavior. If evaluated solely by standard deep learning metrics (Figure 11b), the PINN appeared to reach its optimal state at Epoch 138, where the combined validation loss hit its statistical minimum. However, tracking the independent Mean Physics Error reveals a radically different structural reality (Figure 10c).

International Journal of Engineering Research & Technology (IJERT)
ISSN: 2278-0181
Vol. 15 Issue 05 , May - 2026

Long after the statistical validation loss plateaued, the PINN continued to aggressively refine its internal physical logic, driving the mean structural error continuously downward.

The absolute peak of physical realism was achieved by AI at Epoch 454, for which the mean physics error was at its global minimum value of 986.49 kN. However, as shown in Figure 10d, forcing the optimizer to keep updating weights beyond this optimal checkpoint caused late-stage gradient chaos. Between Epoch 454 and Epoch 500, the physics error violently oscillated, spiking from its minimum of 986 kN back up to over 2,386 kN in just 25 epochs. The oscillation happens because the sharp, very constrained local minima of the physics loss landscape fight with the broader, smoother landscape of the data-driven MSE loss. Ultimately, these learning curves empirically prove that standard early-stopping mechanisms (which monitor validation MSE) are dangerously inadequate for structural engineering AI. PINN architectures require decoupled monitoring; extracting the weights at the exact epoch of minimum physical error (Epoch 454) is mandatory to guarantee structural safety and prevent late-stage mathematical degradation.

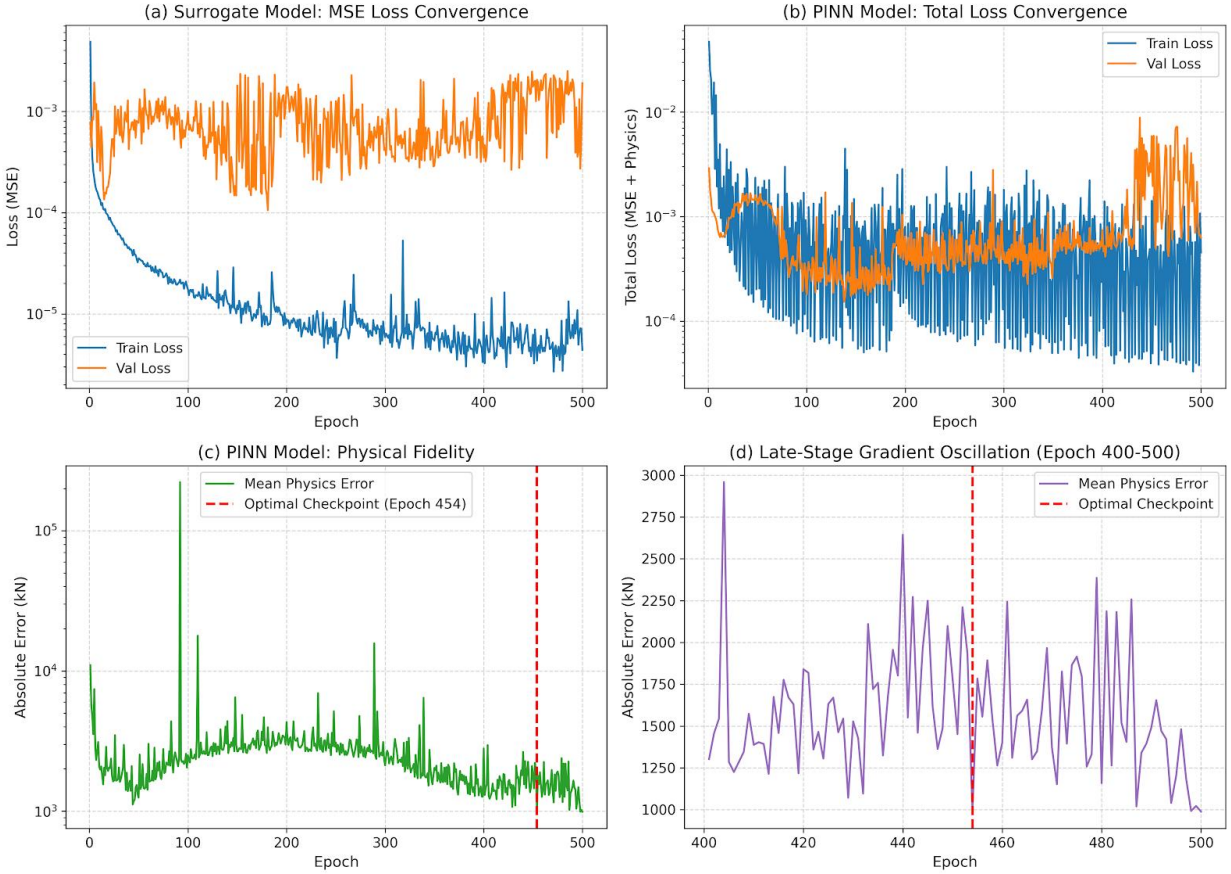

Figure 11: *The Epoch Oscillation Phenomenon*

5.6 Domain Generalization and Low-Density Learning Dynamics (Long Span Architecture)

While the Short Span model was trained on a highly dense parametric grid to achieve maximum precision for common bridge geometries, the Long Span architecture ($L \in [2{,}2000]$ m) was deliberately trained on a lower-density combinatorial space. This low-density training strategy was implemented specifically to act as a robust computational safety net. By exposing the network to extreme, multi-kilometer boundary conditions, it ensures that if a user or automated generative workflow inputs a span strictly exceeding 300 m, the Bridge Information Modeling (BrIM) tool can still return physically viable approximations rather than catastrophic null values or system failures. Analyzing the learning history of this "generalist" Long Span model (Figure 12a,b,c) reveals training dynamics that contrast sharply with the Short Span pipeline. Because the neural networks were tasked with mapping a vastly larger, hyper-dimensional geometric space using fewer, widely distributed data points, the convergence process was significantly prolonged and inherently smoother. For the standard Surrogate model, the validation MSE did not plateau early; it continued a gradual descent, reaching its optimal statistical minimum at Epoch 466.

Similarly, the Physics-Informed Neural Network (PINN) did not experience the aggressive "two-faced" separation between data loss and physics error observed in the Short Span model. The combined data-driven validation loss reached its minimum at Epoch 498, while the fundamental Mean Physics Error reached its absolute minimum just slightly earlier at Epoch 491 (achieving an optimal error of 12,232.83 kN relative to the extreme maximum tension bounds). Furthermore, as illustrated in Figure 12d, the late-stage gradient chaos was virtually nonexistent. The lower density of the training data inherently regularized the loss landscape, preventing the

International Journal of Engineering Research & Technology (IJERT)
ISSN: 2278-0181
Vol. 15 Issue 05 , May - 2026

network from becoming trapped in sharp local minima and allowing the physics constraint to smoothly guide the weights to convergence. This proves that for exceptionally wide structural domains, extending training duration to the full 500 epochs without aggressive early stopping is mathematically justified.

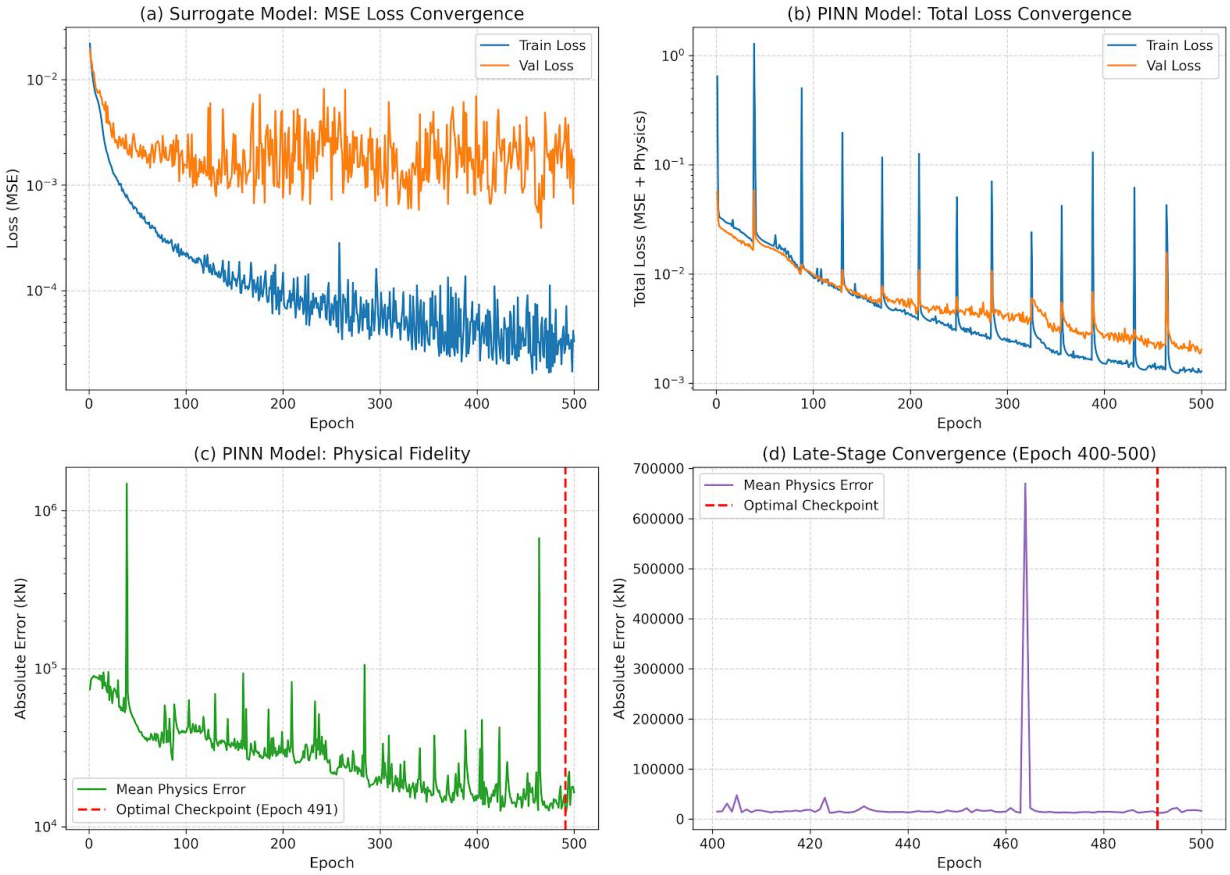

Figure 12: *Low-Density Learning Dynamics*

6. CONCLUSION

This work presents an exhaustive dual-pipeline artificial intelligence framework for tackling the severe computational bottlenecks related to the exact catenary analysis in stress ribbon and cable supported bridges. This paper systematically evaluates conventional data-driven Surrogate models and Physics-Informed Neural Networks (PINNs) for specialized Short Span ($\leq$ 300 m) and Long Span ($\leq$ 2000 m) domains, giving a paradigm shift in real-time, physically reliable structural design. The empirical results show the neural network architectures' ability to achieve breakthrough computational speed-ups, up to 33.36× faster than classical iterative mathematical solvers, while maintaining excellent normalized accuracy (NMAE < 0.55%) in massive, hyper-dimensional design spaces. Moreover, the domain-overlap analysis is a clear proof of the need for a dedicated Short Span pipeline, since it bypasses the localized resolution loss that plagues broad-domain, universal networks.

Most importantly, this work alleviates the fundamental tension between computational speed and structural safety by advocating a complementary dual-model workflow. The Surrogate model is the high-throughput engine for massive-scale parametric screening and the PINN is the ultimate verification engine. The PINN offers intrinsic explainability by incorporating the catenary equilibrium equations directly into the loss function of the neural network. It constrains its predictions by the laws of statics, closing the critical "trust gap" between black-box machine learning and interpretable structural mechanics. Furthermore, the discovery of the "Epoch Oscillation Phenomenon" offers a key operational principle for future researchers: PINN structures need decoupled, physics-error-driven early stopping to avoid mathematical degradation in later stages. The physics-aware models are deployed as a cloud-based computational backend, ultimately unlocking the true potential of Bridge Information Modeling (BrIM). They turn BrIM from a static 3D repository into a dynamic, fully interactive, real-time digital twin. Future work will extend the PINN physics-loss functions to incorporate 3D cable network interactions, asymmetric dynamic loading (e.g., wind flutter and traffic), and the application of "hard" mathematical constraints to ensure zero-residual equilibrium in complex structural topologies.

DATA AVAILABILITY STATEMENT

The data and code that support the findings of this study are openly available to promote reproducible research in computational structural engineering. The synthetic datasets (*ShortSpan_Data.csv, LongSpan_Data.csv*), the PyTorch training scripts (*AITraining.py*), the inference evaluation tools, and the final ONNX model weights (*BEST_surrogate.onnx,*

International Journal of Engineering Research & Technology (IJERT)
ISSN: 2278-0181
Vol. 15 Issue 05 , May - 2026

BEST_pinn.onnx) have been deposited in a public repository. They can be accessed at *https://github.com/thevijayparmar/Stress Ribbon-Bridge-PINN*. The exact mathematical catenary solver used to generate the baseline data is also included in the repository.

ACKNOWLEDGMENT

This study forms a key part of the doctoral research carried out at Gujarat Technological University. The authors thank University for academic guidance and support.

CONFLICTS OF INTEREST

The authors declare that there are no known competing financial interests or personal connections that could have influenced the findings presented in this manuscript.

REFERENCES

[1] Bahadori-Jahromi A, Room S, Paknahad C, Altekreeti M, Tariq Z, Tahayori H. The Role of Artificial Intelligence and Machine Learning in Advancing Civil Engineering: A Comprehensive Review. Applied Sciences 2025, Vol 15, Page 10499 2025;15:10499. https://doi.org/10.3390/APP151910499.

[2] Tita EE, Watanabe G, Shao P, Arii K. Development and Application of Digital Twin–BIM Technology for Bridge Management. Applied Sciences 2023, Vol 13, Page 7435 2023;13:7435. https://doi.org/10.3390/APP13137435.

[3] Sacks R, Brilakis I, Pikas E, Xie HS, Girolami M. Construction with digital twin information systems. Data-Centric Engineering 2020;1:e14. https://doi.org/10.1017/DCE.2020.16.

[4] Li K, Li H, Khuddair A, Dong Y, Wang J. An end-to-end and high accuracy solution of cable catenary using dual-parameter optimized physics-informed neural networks 2025:282–9. https://doi.org/10.17868/STRATH.00093245.

[5] Beivydas E, Juozapaitis A. Experimental and Numerical Analysis of an Innovative Combined String–Cable Bridge. Applied Sciences (Switzerland) 2024;14. https://doi.org/10.3390/APP14177542.

[6] Chen Y, Lin C, Sui H, Okauchi R, Akita A, Chun* P. Automated generation of IFC-compliant bridge information models from structured design data. Journal of Information Technology in Construction (ITcon), 31, 420-438 Http://WwwItconOrg/2026/19 2026;31:420–38. https://doi.org/10.36680/J.ITCON.2026.019.

[7] Shim CS, Roh GT. Data-driven modeling algorithms for cable-stayed bridges considering mechanical behavior. Applied Sciences (Switzerland) 2021;11:1–22. https://doi.org/10.3390/APP11052266.

[8] Wang H, Song Y, Yang H, Liu Z. Generalized Koopman Neural Operator for Data-Driven Modeling of Electric Railway Pantograph–Catenary Systems. IEEE Transactions on Transportation Electrification 2025;11:14100–12. https://doi.org/10.1109/TTE.2025.3609347.

[9] Luqman M, Arif M. Physics-Informed Neural Networks Fusion with Deep Learning for Structural Health Monitoring and Prognostics - A Review 2026:75–83. https://doi.org/10.4028/P-LSQL3S.

[10] Yu X, Wan X, Nie J, Song G, Yu A, Yu J. Real-Time Mechanical Modeling for Bridge Construction Based on Digital Twins and Parameter Inversion. Applied Sciences 2026, Vol 16, Page 2920 2026;16:2920. https://doi.org/10.3390/APP16062920.

[11] Hagen A, Andersen TM. Asset management, condition monitoring and Digital Twins: damage detection and virtual inspection on a reinforced concrete bridge. Structure and Infrastructure Engineering 2024;20:1242–73. https://doi.org/10.1080/15732479.2024.2311911.

[12] Hassija V, Chamola V, Mahapatra A, Singal A, Goel D, Huang K, et al. Interpreting Black-Box Models: A Review on Explainable Artificial Intelligence. Cognitive Computation 2023 16:1 2023;16:45–74. https://doi.org/10.1007/S12559-023-10179-8.

[13] Aziz MT, Osabel DM, Kim Y, Kim S, Bae J, Tsavdaridis KD. State-of-the-art artificial intelligence techniques in structural engineering: A review of applications and prospects. Results in Engineering 2025;28. https://doi.org/10.1016/J.RINENG.2025.107882.

[14] Zaker Esteghamati M, Wang J, Wang X, Paal S, Murphy J, Namin A, et al. Making the Black Box Transparent: State of the Art in Explainable Machine Learning for Structural Design and Assessment 2025. https://doi.org/10.31224/5141.

[15] Kurcjusz M, Das RR. Advances in structural engineering through artificial intelligence: methods, challenges and opportunities. Acta Scientiarum Polonorum Architectura 2025;24:418–30. https://doi.org/10.22630/ASPA.2025.24.28.

[16] Thawon I, Vo D, Bui TQ, Rattanamongkhonkun K, Chamroon C, Tippayawong N, et al. Physics-Informed Neural Networks: Current Progress and Challenges in Computational Solid and Structural Mechanics. Computer Modeling in Engineering & Sciences 2026;146. https://doi.org/10.32604/CMES.2026.077044.

[17] Raissi M, Perdikaris P, Karniadakis GE. Physics-informed neural networks: A deep learning framework for solving forward and inverse problems involving nonlinear partial differential equations. J Comput Phys 2019;378:686–707. https://doi.org/10.1016/J.JCP.2018.10.045.

[18] Cuomo S, Di Cola VS, Giampaolo F, Rozza G, Raissi M, Piccialli F. Scientific Machine Learning Through Physics–Informed Neural Networks: Where we are and What's Next. Journal of Scientific Computing 2022 92:3 2022;92:88-. https://doi.org/10.1007/S10915-022-01939-Z.

[19] Tahimi A. Physics-Informed Neural Networks: A Didactic Derivation of the Complete Training Cycle 2026.

[20] Sukumar N, Roy R. A Wachspress-based transfinite formulation for exactly enforcing Dirichlet boundary conditions on convex polygonal domains in physics-informed neural networks 2026.

[21] Sunil P, Sills RB. FE-PINNs: finite-element-based physics-informed neural networks for surrogate modeling 2024. https://doi.org/10.1063/5.0299671.

[22] Liu J, Li Y, Sun L, Wang Y, Luo L. Physics and data hybrid-driven interpretable deep learning for moving force identification. Eng Struct 2025;329:119801. https://doi.org/10.1016/J.ENGSTRUCT.2025.119801.

[23] Yee B, Collins W, Pellegrini B, Wang C. Meta-learning physics-informed neural networks for few-shot parameter inference 2025. https://doi.org/10.21203/RS.3.RS-7497594/V1.

[24] Mish: A Self Regularized Non-Monotonic Neural Activation Function n.d. https://www.researchgate.net/publication/335395448_Mish_A_Self_Regularized_Non-Monotonic_Neural_Activation_Function (accessed May 12, 2026).

[25] Kingma DP, Ba JL. Adam: A Method for Stochastic Optimization. 3rd International Conference on Learning Representations, ICLR 2015 - Conference Track Proceedings 2014.

[26] Abdollahi A, Li D, Deng J, Amini A. An explainable artificial-intelligence-aided safety factor prediction of road embankments. Eng Appl Artif Intell 2024;136. https://doi.org/10.1016/J.ENGAPPAI.2024.108854.

[27] Honghong S, Gang Y, Haijiang L, Tian Z, Annan J. Digital twin enhanced BIM to shape full life cycle digital transformation for bridge engineering. Autom Constr 2023;147. https://doi.org/10.1016/J.AUTCON.2022.104736.

[28] Lu Q, Xie X, Parlikad AK, Schooling JM, Konstantinou E. Moving from building information models to digital twins for operation and maintenance. Proceedings of the Institution of Civil Engineers: Smart Infrastructure and Construction 2021;174:46–56. https://doi.org/10.1680/JSMIC.19.00011.

[29] Akbarnezhad M, Salehi M, DesRoches R. Application of machine learning in seismic fragility assessment of bridges with SMA-restrained rocking columns. Structures 2023;50:1320–37. https://doi.org/10.1016/J.ISTRUC.2023.02.105.